

Structure–Affinity Relationship Study of Bleomycins and Shble Protein by Use of a Chemical Array

Isao Miyazaki,^[a] Hideo Okumura,^[a] Siro Simizu,^[a] Yoshikazu Takahashi,^[b] Naoki Kanoh,^[a, c] Yasuhiko Muraoka,^[b] Yoshiaki Nonomura,^[b] and Hiroyuki Osada*^[a]

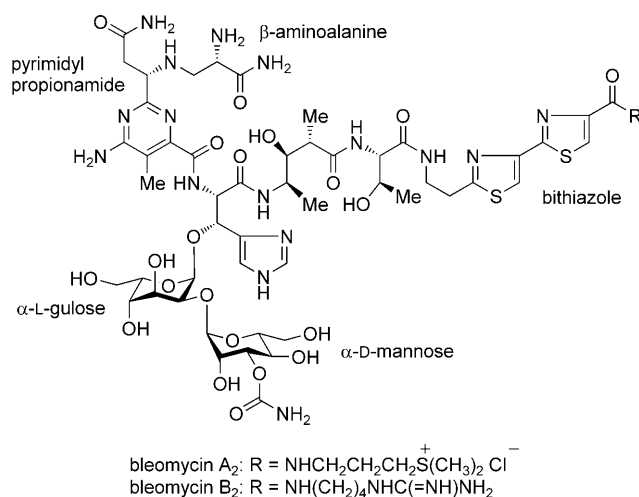
The photocrosslinked chemical array format is useful not merely for screening protein ligands, but also for gaining insight into structure–affinity relationships (SARs). By probing an array of 2000 natural products, containing 50 bleomycin (BLM) derivatives, with cell lysates that overexpress RFP-fused Shble protein, we successfully observed interactions between Shble protein and BLMs on the array. Among the BLM derivatives, those that had long C-terminal tails were found to bind strongly. The binding signal intensities observed on the chemical array correlated well with the association constants, which

were determined by isothermal titration calorimetry (ITC) experiments ($r^2 = 0.663$), showing that the on-chip results were not an artifact of ligand immobilization. In addition to the C-terminal tails, the propionamide moieties in pyrimidoblastic acid (PBA) also appeared to be important for binding. The contributions of the propionamide moieties of PBA to binding were further supported by the X-ray structure of the complex of Shble protein and BLM A₆. These results provide insight into the structural requirements for recognition of BLMs by Shble protein.

Introduction

Bleomycins (BLMs) are a family of glycopeptide antibiotics that have been isolated from several *Streptomyces* species.^[1,2] The structure was proposed in 1978^[3] and finally confirmed by Takita et al.^[4,5] and Hecht et al.^[6] The chemotherapeutic formulation of BLM, which is primarily composed of BLM A₂ and BLM B₂ (Scheme 1), has been widely used in combination with

The lethal effect of BLMs is thought to be harmful not only for cancer cells but also for BLM-producing microorganisms. Therefore, to protect themselves from the lethal effects of their own products, microorganisms produce proteins to modify and to sequester the drug. As one example, *Streptomyces verticillius*, a BLM producer, is known to harbor the *blmA* and *blmB* genes, which encode for a BLM-binding protein (BlmA)^[10] and an N-acetyl transferase (BlmB),^[11] respectively. In addition, a gene that encodes a small acidic BLM-binding protein, Shble protein, has been cloned from the BLM-producing *Streptoalloeus hindustanus*.^[12,13] Although BLMs have not been used as antibacterial agents, many clinically isolated strains of methicillin-resistant *Staphylococcus aureus* (MRSA) produce BLM-binding proteins that sequester these antibiotics, leading these strains to be resistant to BLMs at high levels. Sugiyama et al. have reported that many strains of clinically isolated MRSA are resistant to BLMs and that the mechanism of the resistance is due to the existence of a BLM-binding protein, designated BlmS.^[14] Another BLM-binding protein, designated BlmT, has been found in *E. coli*.^[15]



Scheme 1. Structures of bleomycins A₂ and B₂.

other chemotherapeutic agents^[7,8] for the treatment of skin, head, and neck carcinomas. The biological activity of BLMs is thought to originate from their DNA-damaging capacities: Fe^{II}-complexed BLMs have been reported to cause sequence-specific DNA cleavage in the presence of oxygen.^[9]

[a] I. Miyazaki, Dr. H. Okumura, Dr. S. Simizu, Dr. N. Kanoh, Prof. H. Osada
 Antibiotics Laboratory and Chemical Biology Department, RIKEN
 2–1 Hirosawa, Wako, Saitama 351-0198 (Japan)
 Fax: (+81) 48-462-4669
 E-mail: hisyo@riken.jp

[b] Dr. Y. Takahashi, Dr. Y. Muraoka, Dr. Y. Nonomura
 Microbial Chemistry Research Center
 Tokyo 141-0021 (Japan)

[c] Dr. N. Kanoh
 Graduate School of Pharmaceutical Sciences, Tohoku University
 Sendai, Miyagi 980-8578 (Japan)

Supporting information for this article is available on the WWW under
<http://dx.doi.org/10.1002/cbic.200800728>.

It has been shown that transgenic expression of *Shble* protein or adenovirus-mediated transfer of the *Shble* gene prevents BLM-induced pulmonary fibrosis.^[16,17] An analysis of the mechanism of binding between BLMs and these proteins is thus important for understanding of the fundamental role of resistance proteins and for the rational design of pharmaceutical drugs that have better clinical efficacy and lower toxicity.

We have developed a nonselective photo-immobilization method to introduce a variety of small molecules onto glass slides.^[18–20] We showed that the resulting photocrosslinked chemical arrays were useful not merely for protein ligand screening but also for gaining insight into structure–affinity relationships (SARs): that is, the relationship between structural motifs that are found in small molecules and their binding affinities for proteins of interest. Because very small sample amounts are needed to construct the microarray and because the photo-immobilization method can be applied to complex natural products, the photocrosslinked chemical array platform is well suited for evaluation of the SARs between *Shble* protein and BLMs.

In this work we have evaluated the binding abilities of various BLMs with *Shble* protein by using photocrosslinked chemical arrays. The on-chip fluorescence signals indicated that BLM derivatives that have a C-terminal tail connected to the bithiazole moiety and that contain propionamide moieties of pyrimidoblastic acid (PBA) tend to bind strongly to *Shble* protein. To confirm these results, we performed isothermal titration calorimetry (ITC) measurements and determined the thermodynamic properties of the interactions between *Shble* protein and representative BLM derivatives. Finally, we obtained a co-crystal structure of the *Shble* protein/BLM A₆ complex to assess the importance of the two described motifs in the recognition events between BLMs and *Shble* protein.

Results

Shble protein binds specifically to a particular class of BLM derivatives on chemical arrays

In 2006, Schreiber et al. reported that mammalian cell lysates that overexpressed a green fluorescent protein (GFP)-fused protein could be used for binding assays based on chemical arrays.^[21] We have adopted this system and modified it to create a ligand-screening method that enables us easily to distinguish false positives from hit signals.^[22] We hence set out to use this system to study the SARs of BLMs and *Shble* protein on photocrosslinked chemical arrays. To this end, we constructed photocrosslinked chemical arrays on which 2000 unique, natural-product-based compounds, containing 50 BLM derivatives, were photochemically immobilized (see the Supporting Information S1). Photogenerated carbene is known to react with a variety of single and multiple bonds,^[23] and immobilization on our chemical array platform took place in a functional-group-independent manner.^[18–20] Also, two lines of HEK293T cells, which overexpressed red fluorescent protein (RFP) or RFP-fused *Shble* (RFP-*Shble*) protein, were created. Two chemical array slides were independently treated with RFP-*Shble* pro-

tein-overexpressing cell lysates and RFP-overexpressing cell lysates. To differentiate *Shble* protein binding signals, a fluorescent image of the RFP-*Shble* protein-treated slide was colored

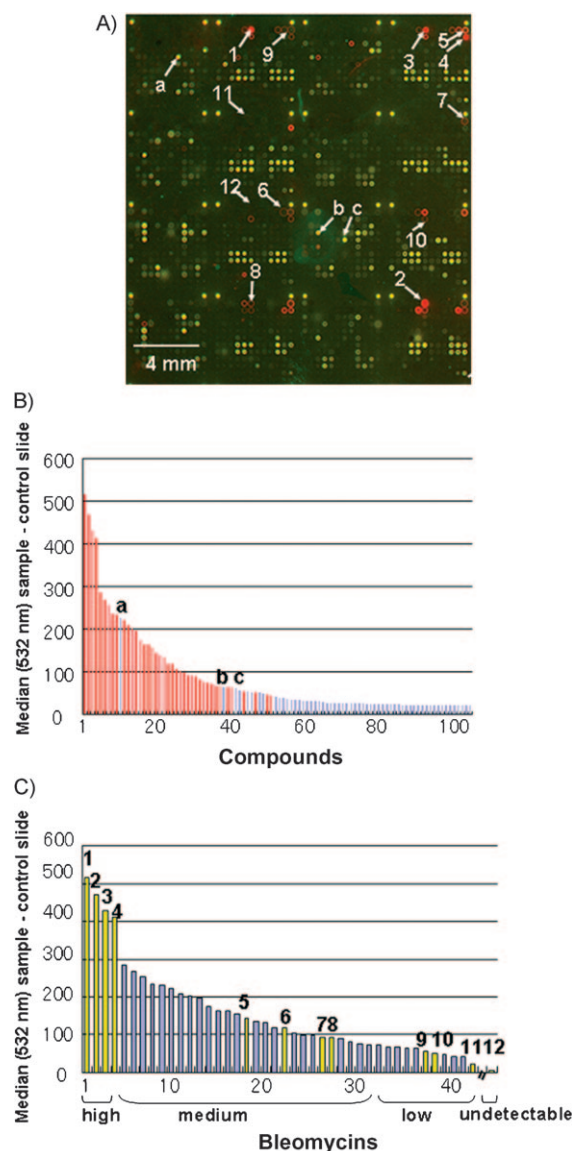


Figure 1. On-chip binding assay on cell lysates overexpressing RFP-fused *Shble* protein. A) 2000 natural products, including 50 bleomycin derivatives, were immobilized on a glass slide. The HEK293T cell lysates expressing RFP or RFP-fused *Shble* protein were incubated with the slides, and the slides were briefly washed and scanned. The slides treated with RFP-fused *Shble* protein (sample) and with RFP (control) were colored red and green, respectively. The merged image is shown. Bleomycin derivatives 1–12 are indicated with white arrows. B) One hundred selected compounds and their fluorescence signals at 532 nm. Compounds were selected according to signal intensity and are listed in descending manner. Fluorescence signal at 532 nm is determined by subtracting the F_{532} control slide median from the F_{532} sample slide median. Bleomycin derivatives are shown as red bars. These data were calculated from averages of duplicate positions on a slide. C) Plot of fluorescence intensities of the bleomycin derivatives, listed in descending manner. To verify the differences reflecting the compounds' binding affinities towards *Shble* protein, 12 compounds were selected from four classes (high, medium, low, and undetectable). The four classes were determined by fluorescence signals at 532 nm: high means >300, medium means 300–70, low means 70–20, and undetectable means <20.

in red, the RFP-treated slide was colored in green, and the images were merged. The merged image is shown in Figure 1A. Hence, red signals in the merged images indicate the presence of RFP-Shble that is specifically bound to the area.

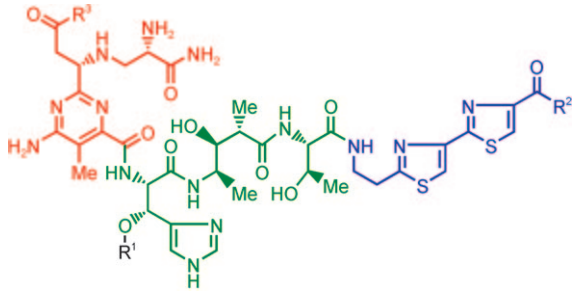
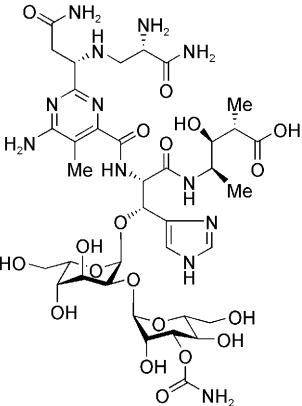
All of the red signals that were observed in Figure 1A were localized to BLM derivatives. The yellow signals that were detected were primarily derived from the position marker rhodamine and from fluorescent molecules that were immobilized on the array. Many anthracyclines and angucyclines were included in our library, and these were identified as yellow spots in the merged image (some compounds are shown in Table S1 and Figure S2 in the Supporting Information).

To show the results in a quantitative manner, the top 100 RFP-Shble-derived fluorescence values [F_{532} median (sample) – F_{532} median (control)] of the immobilized compounds are listed in descending manner as shown in Figure 1B. Although nearly all of the strong signals were found for BLMs (red bars), significant signals were also observed for other compounds

(blue bars). However, when the merged image was carefully analyzed, these compounds were determined to be yellow spots (for example, compounds a–c in Figure 1A). Accordingly, we concluded that Shble protein binds specifically to BLM derivatives.

When the fluorescence signals from BLM derivatives were selected and listed in order of magnitude, it was clear that there were significant differences between the fluorescence intensities of the BLMs (Figure 1C). We classified the BLM derivatives in Figure 1C into four categories (high, medium, low, and undetectable) according to fluorescence intensity, and structural features were carefully evaluated (see the Supporting Information for the structures of the BLMs). Representative BLM derivatives (1–12) in these four categories were chosen and are listed in Table 1. Basically, a BLM molecule can be dissected into five structural domains: 1) the pyrimidoblastic acid (PBA) subunit (red part in Table 1), 2) the (2S,3S,4R)-4-amino-3-hydroxy-2-methylpentanoic acid (AHM) subunit and the hydroxy-

Table 1. Structures of the selected compounds 1–12. Each is complexed with a copper atom.

| Compound ID | R ¹ | R ² | R ³ | Names | On-chip categories |
|-------------------------------------------------------------------------------------|-------------------------------------------------------------------------------------|---------------------------------------------------------------------------------------------------------------------------|-----------------|-----------------------------------|--------------------|
|  | | | | | |
| 1 | 3-carbamoyl- α -D-mannose and α -L-gulose | NH(CH ₂) ₃ NH(CH ₂) ₃ NH(CH ₂) ₃ NHC(=NH)cyclohexyl | NH ₂ | – | high |
| 2 | 3-carbamoyl- α -D-mannose and α -L-gulose | NH(CH ₂) ₃ NH(CH ₂) ₃ NH(CH ₂) ₃ NH ₂ | NH ₂ | bleomycin A ₆ | high |
| 3 | 3-carbamoyl- α -D-mannose and α -L-gulose | NH(CH ₂) ₃ NH(CH ₂) ₄ NH ₂ | NH ₂ | bleomycin A ₅ | high |
| 4 | 3-carbamoyl- α -D-mannose and α -L-gulose | NH(CH ₂) ₃ NH(CH ₂) ₄ NH(CH ₂) ₃ NHCOCH ₃ | NH ₂ | – | high |
| 5 | 3-carbamoyl- α -D-mannose and α -L-gulose | NH(CH ₂) ₄ NHC(=NH)NH ₂ | NH ₂ | bleomycin B ₂ | medium |
| 6 | 3-carbamoyl- α -D-mannose and α -L-gulose | NHC ₆ H ₄ (p-CH ₂ N(CH ₃) ₂) | NH ₂ | – | medium |
| 7 | 3-carbamoyl- α -D-mannose and α -L-gulose | NH(CH ₂) ₃ SCH ₃ | NH ₂ | bleomycin demethyl A ₂ | medium |
| 8 | 3-carbamoyl- α -D-mannose and α -L-gulose | NH ₂ | NH ₂ | bleomycin B ₁ | medium |
| 9 | 3-carbamoyl- α -D-mannose and α -L-gulose | OH | NH ₂ | bleomycinic acid | low |
| 10 | H | NH(CH ₂) ₄ NHC(=NH)NH ₂ | NH ₂ | bleomycin aglycon B ₂ | low |
| 11 | 3-carbamoyl- α -D-mannose and α -L-gulose | NH(CH ₂) ₄ NHC(=NH)NH ₂ | OH | dll-bleomycin B ₂ | low |
| 12 |  | | | | |

histidine subunit (green part), 3) the bithiazole moiety (blue part), 4) the sugar moiety (R^1) composed of 3-carbamoyl- α -D-mannose and α -L-gulose, and 5) the C-terminal tail attached to the bithiazole (R^2). The PBA and AHM subunits, as well as the bithiazole moiety, together comprise a common backbone of BLM. All of the *Shble* protein-bound BLM derivatives on our chemical array slide possess this common backbone, indicating that this structure is necessary for recognition by *Shble* protein. Of the five domains, the bithiazole moiety is thought to be essential for *Shble* protein binding; none of the derivatives not containing the bithiazole moiety was included in detectable categories (high, medium, low) in Figure 1C, although there were such derivatives present on the arrays (data not shown). This finding was also supported by the fact that phleomycins, which have only one thiazole ring, showed binding signals at low levels (see compound **G** in Table S1 and Figure S2). It should be noted that a small structural change in the PBA subunit (compound **5** vs. **11**) made a significant difference in binding signal (Figure 1A and C). The sugar component and the C-terminal tail connected to the bithiazole moiety are probably not essential for binding, because derivatives **8–10** did generate any binding signals. However, the C-terminal tail did seem to modulate binding, because many BLM derivatives that generated high or medium signal intensities—including all of the top four compounds (**1–4**)—have relatively long tails containing amino groups at the C-termini (Figure 1C and D). These findings indicate that long chains that contain amino groups can have positive effects on BLM/*Shble* protein interaction.

ITC analysis of *Shble* protein binding to various BLM derivatives

To confirm the results obtained from the on-chip SAR study, we performed isothermal titration calorimetry (ITC) measurements to determine the thermodynamic parameters of the interactions between *Shble* protein and BLM derivatives. To this end, His₆-*Shble* protein was expressed in *E. coli* and purified. Compounds **1–12** were used primarily because of the limited availabilities of the other derivatives. The association constants (K_a) that were obtained for compounds **1–12** by ITC measurement are summarized in Table 2. Compound **1**, which gave the strongest binding signal in the chemical array experiments, generated the largest K_a value ($1.28 \times 10^8 \text{ M}^{-1}$) out of the tested samples. This value is larger than that of BLM A₂ ($2 \times 10^7 \text{ M}^{-1}$),^[24]

indicating that compound **1** is the tightest *Shble* protein-binder known. Compounds **2–5**, all of which possess long, amine-containing C-terminal tails at their R^2 positions, also had strong affinities to *Shble* protein ($4.27\text{--}7.72 \times 10^7 \text{ M}^{-1}$). In particular, compound **5** showed a >70-fold higher binding affinity than compound **11**, which differed from **5** at the R_3 position. Compound **10** had a K_a value of $7.64 \times 10^6 \text{ M}^{-1}$, implying that the replacement of the sugar moieties at the R^1 position appeared to be tolerant to binding.

On the other hand, compound **12** did not bind *Shble* protein at all. Compound **12** possesses the common backbone that is known to play an important role in the efficiency of DNA cleavage,^[25] but in this case we concluded that this backbone only served as a connection between bithiazole and the PBA subunit and that the backbone did not generate sufficient binding networks to stabilize the complex.

Importantly, the binding constants that were determined by the ITC experiments correlated well with the binding signal intensities that were observed on the chemical array ($r^2 = 0.663$; Figure 2). This result showed that the on-chip results were not an artifact of ligand immobilization.

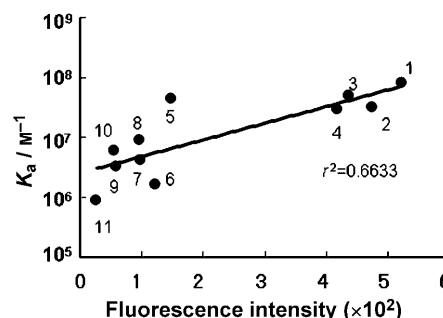


Figure 2. Correlation between binding constants (K_a) obtained from ITC experiments and fluorescence signals observed on the chemical arrays. The x-axis represents the fluorescence intensities of compounds **1–11** on the glass slide (Figure 1C). The y-axis represents the K_a values calculated by ITC analysis (Table 2). $r^2 = 0.6633$.

Crystal structure analysis of wild-type *Shble* protein in complex with BLM

We succeeded in solving an X-ray crystal structure of *Shble* protein in complex with BLM A₆ (**2**) at 1.6 Å (Figure 3). The crystals that were grown belong to space group $P2_12_12_1$, with unit cell parameters of $a = 40.0 \text{ Å}$, $b = 53.9 \text{ Å}$, and $c = 125.5 \text{ Å}$. Like the previously reported^[26,27] BLM-binding protein structures, the current model contains two monomeric *Shble* protein molecules and two molecules of **2** in the asymmetric unit (2:2 complex; Figure 3A).

The bithiazole moiety of **2** is located along the large groove that is formed at the interface of two *Shble* protein molecules, and the two thiazolium rings interact with Phe33B,^[28] Phe38B, and Trp102A through hydrophobic interactions (Figure 3B).

It has been proposed that these stacking effects contribute to stabilization of the binding of **2** to *Shble* protein. Electron density for the C-terminal tail of **2** is absent from the binary

Table 2. Binding constants of **1–12** to *Shble* protein as determined by ITC analysis.

| Compound | $K_a [\text{M}^{-1}]$ | Compound | $K_a [\text{M}^{-1}]$ |
|-----------|-----------------------|-----------|-----------------------|
| 1 | 1.28×10^8 | 2 | 4.71×10^7 |
| 3 | 7.72×10^7 | 4 | 4.27×10^7 |
| 5 | 6.84×10^7 | 6 | 1.82×10^6 |
| 7 | 5.19×10^6 | 8 | 1.18×10^7 |
| 9 | 3.91×10^6 | 10 | 7.64×10^6 |
| 11 | 9.45×10^5 | 12 | N.B. ^[a] |

[a] No binding under the ITC measurement conditions.

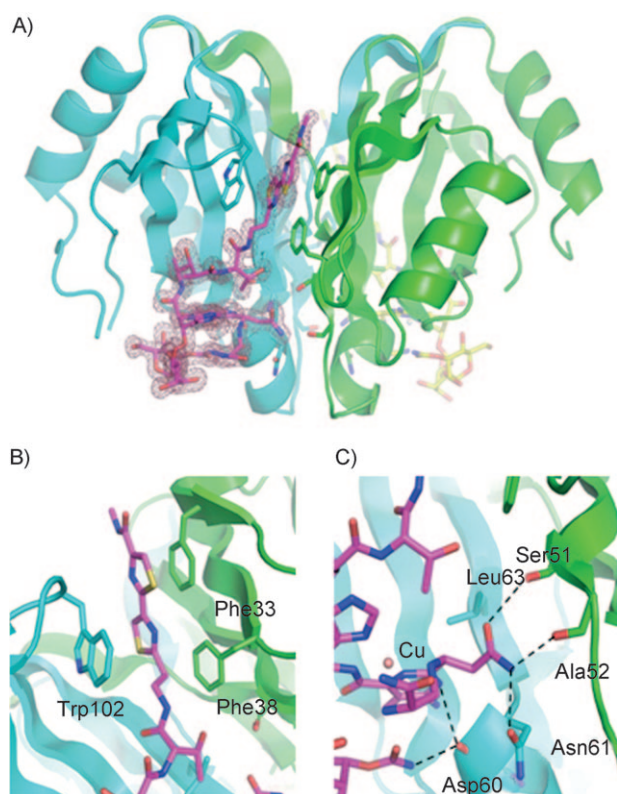


Figure 3. Crystal structure of the complex formed by *Shble* protein and compound **2**. A) Overall view of the complex formed by *Shble* protein and compound **2**. Each *Shble* monomer is colored in blue (subunit A) or green (subunit B). Two **2** molecules are drawn in magenta and yellow. Electron density around **2** is contoured at 1.0σ . B) The binding of **2** to *Shble* protein in the long groove. A molecule of **2** and the surrounding residues of *Shble* protein are shown in stick representation. The bithiazole moiety of **2** is stabilized by a stacking interaction. C) Hydrogen-bonding network between *Shble* protein and the terminal amide group of the pyrimidobranic acid moiety of **2**. The carbon atoms of **2** and copper ion are colored magenta and brown, respectively. Each subunit of *Shble* protein is colored as in (B).

complex structure. Collectively, these data suggest a disordered conformation of the tail end.^[29] The propionamide moiety of the PBA subunit in **2** forms hydrogen bonds with the Ser51B hydroxy group and the Ala52B carbonyl oxygen (Figure 3C). As described above, the differences between the K_a values of **5** and **11** (Figure 2D) indicate that this hydrogen-bonding network contributes robustly to stabilization of the *Shble* protein/BLM complex. It also has been suggested that changing the amide moiety to a carboxylic acid moiety should not only lose the hydrogen-bonding network for stabilization but also induce repulsion between the negatively charged carboxylate group and the Ala52B carbonyl oxygen or Ser51B hydroxy group.

Discussion

Several crystal structures of ligand–BLM binding protein complexes, including BlmT/BLM A₂,^[24] BlmA/Cu^{II}-bound or -unbound BLM A₂,^[29,30] thermostable *Shble* mutant/BLM A₂,^[27] as well as solution structure of *Shble*/Zn^{II}-bound BLM,^[31] have so far been reported. These crystallographic and NMR analyses

present detailed depictions of drug–protein interactions, but it is still difficult to evaluate the relative and quantitative importance of individual functional groups on the complex drug molecule for the interaction. Many BLM derivatives have been identified or synthesized^[32–38] to obtain these information, but there are few available data relating to binding patterns of a large number of BLM analogues.

Through our SAR analysis with a photocrosslinked chemical array platform, we found that all of the *Shble*-bound BLMs have a common backbone, made up of the PBA, AHM, and bithiazole units. The analysis also suggested the importance of the bithiazole moiety, the propionamide moiety of the PBA subunit, and the C-terminal tail that is connected to bithiazole during binding. This hypothesis was confirmed by ITC experiments.

The importance of the bithiazole moiety in the interaction between BLM and BLM-binding proteins has been suggested by X-ray crystallographic and NMR analyses.^[27,29,31] Our on-chip SAR, as well as the ITC experiments, clearly showed that the stacking effect of the bithiazole moiety with aromatic residues in the *Shble* protein was critical, because derivatives that lacked the bithiazole did not generate positive binding signals on the chemical arrays; moreover, compound **12** did not bind to *Shble* protein at all in the ITC experiment.

The hydrogen-bonding networks that surround the PBA domain of BLMs in co-crystal structures have been observed in previous analyses, but the quantitative importance of the propionamide group in the PBA domain has not been assessed. It is noteworthy that our study demonstrated a >70-fold decrease in affinity when the amide moiety in the propionamide group was altered to a carboxylic acid. This result is probably due to loss of two hydrogen bonds with Ala52 and Asn61 (Figure 3C).

The C-terminal tail moiety (R^2 in Table 1) attached to the bithiazole group has been reported to contribute to BLM–DNA interaction.^[39] No electron density map of this tail has been clarified by any reports,^[24,27,29,31] and the structure of this tail was also unclear in our crystallographic study (Figure 3A). It has been shown previously that the negatively charged cleft runs between two protein subunits in the *Shble* dimer, suggesting that there are interactions between the positively charged C-terminal tail moiety and the negatively charged residues of resistant proteins (for example, Asp32 in *Shble* protein) and that the terminus is necessary for ligand recognition of the protein but not for ligand stabilization.^[26,29,31] However, results obtained from our study of the SARs of BLMs' binding specificities toward *Shble* protein clearly demonstrated that the tails did modulate the stabilities of the protein–ligand complexes.

The on-chip SAR method described in this study provides valuable insights into the structural requirements for BLMs to be recognized by *Shble* protein in a high-throughput manner. For example, compounds **5** and **11**, which are structurally similar BLMs, were clearly distinguished by their fluorescence signals on the arrays. The chemical array screening method enables SAR analysis with very small amounts of compounds (≤ 10 mM, 1 nL per spot) and cell lysates that express a tagged

protein of interest, whereas both ITC and X-ray crystallography require highly purified and large amounts of proteins.

On the other hand, while the photocrosslinked chemical array platform has proven to be useful, we recognize that the results that were obtained from our on-chip SARs are not definitive. Compounds **5** and **6**, for example, showed similar binding signals on the arrays, whereas ITC analysis showed the binding of **5** to Shb1e protein to be 40 times stronger than that of **6**. One possible reason could be the reactivity of the R² moiety: these compounds differ only in the R² group, thus making it possible that an electron-rich *p*-(dimethylaminomethyl)aniline moiety in compound **6**, which does not participate in binding, could react preferentially with electron-deficient carbene species during the photocrosslinking process. We are currently analyzing the reactivity of the carbene towards a variety of functional groups under our photocrosslinking conditions. The studies should be useful in revealing the origins of these inconsistencies and in providing an array system that is more compatible with evaluations of SAR studies of binding between immobilized compounds and target proteins.

Conclusions

In this study we have performed an analysis of the SARs of BLM derivatives and Shb1e protein by using a chemical array platform, and we suggest that several domains are important for BLM derivatives to be recognized by Shb1e protein. Our hypothesis was confirmed by ITC and X-ray crystallographic analyses. The information that was obtained in this study has provided us with additional insights into the mechanisms of Shb1e protein sequestration, which should become the molecular basis for the design of clinical drugs with better clinical efficacy in the near future.

Experimental Section

Preparation of photocrosslinked chemical array: The slides were prepared as in our previous reports.^[18,19] A solution of the 2000-natural product library (10 mM in DMSO) from the Microbial Chemistry Research Center (Japan) was arrayed onto the photoaffinity linker-coated glass slides. The slides were then exposed to UV irradiation (4 J cm⁻²) at 365 nm by using a CL-1000 L UV crosslinker (UVP, CA). They were rinsed with DMSO, washed successively with DMSO, DMF, THF, DMSO, and Milli-Q water (1 h each), and dried. The slides were degassed and stored at -20 °C until use.

Preparation of mammalian cell lysates expressing RFP-fused Shb1e protein: *Streptococcus hindustanus* Shb1e gene from the pZeoSV2 (+) vector (Invitrogen, Tokyo, Japan) was subcloned into pDsRed-Express-N1 (Clontech, Mountain View, CA). Sequences were confirmed by the dideoxynucleotide chain termination procedure with an automated sequencer (Applied Biosystems). HEK293T cells were cultured in RPMI-1640 medium supplemented with fetal bovine serum (10%) under a humidified atmosphere containing CO₂ (5%). RFP-fused Shb1e protein-expressing cells were created by transfection of the plasmids into exponentially growing HEK293T cells in the presence of the Effectene transfection reagent (Qiagen, Tokyo, Japan). After transient transfection for 24 h, the cells were washed, harvested, suspended in phosphate-buffered saline (PBS), and lysed by sonication. The lysates were centrifuged at

15000 rpm for 15 min, and the amount of protein in each lysate was measured by staining the proteins with Coomassie Brilliant Blue G-250 (BioRad, Hercules, CA). In this paper, the fused Shb1e protein expressed from pDsRed-Express-N1 is designated as RFP-fused Shb1e protein.

Treatment of glass slides with cell lysates and scanning of slides for fluorescence: Glass slides were incubated for 1 h at 30 °C with cell lysates that overexpressed the RFP-fused Shb1e protein or RFP protein (3–4 mg protein per mL) followed by the merged display method.^[22] After incubation, the slides were washed three times, dried, and scanned at 532 nm on a GenePix microarray scanner (Amersham Biosciences). The fluorescence signals were quantified by using GenePix 5.0 software. For the images from each slide, one that was treated with cell lysates that overexpressed RFP was used as control, and the other was incubated with cell lysates overexpressing the RFP-fused Shb1e protein. These were colored green and red, respectively, by using Photoshop 5.5 software. The colored figures were then merged.

Purification of Shb1e protein and isothermal titration calorimetry (ITC): The gene encoding Shb1e protein was subcloned into the pRSET C vector (Invitrogen). An *E. coli* strain—BL21 (DE3)—was transformed with the resulting vector. The transformed cells were cultured in LB medium and lysed by sonication in PBS. Cell lysates were prepared by centrifugation, and Ni-NTA agarose (Qiagen) was added to the cell lysates. The Ni-NTA agarose was washed with PBS, and Ni-NTA agarose-bound His₆-Shb1e protein was eluted with PBS containing imidazole (300 mM). The eluted fractions were then dialyzed with PBS. ITC was performed at 20 °C by use of MicroCal VP-ITC (MicroCal, Northampton, MA). His₆-Shb1e protein was degassed for 3 min before being loaded into a calorimeter cell. A ligand solution (200 μM) in PBS that had been degassed for 3 min before use was titrated with protein (18 μM) in the same buffer. After an initial dummy injection of 2 μL, ligand solution (6 μL) was injected into the calorimeter cell. The resulting titration curves were then processed and fitted with the aid of Origin 7 software. Compounds **2**, **3**, **5**, and **7–11** were isolated from *Streptomyces* and synthesized as described previously.^[35–38,40]

Purification and crystallization of Shb1e protein: For purification of the Shb1e protein, an *E. coli* strain—BL21—harboring nontagged recombinant Shb1e protein was grown in LB medium containing ampicillin (50 μg mL⁻¹). The harvested cells, collected by centrifugation, were extracted by sonication with buffer [Tris-HCl (pH 7.4, 20 mM), PMSF (1 mM), benzamidine (5 mM)]. The resulting supernatant was collected by centrifugation at 40000g for 1 h. The cleared supernatant was applied to a RESOURCE Q column (GE Healthcare) that was equilibrated with Tris-HCl buffer (pH 7.4, 20 mM) and eluted with Tris-HCl buffer (pH 7.4, 20 mM) containing NaCl (0–1 M) in a linear concentration gradient. The fractions containing Shb1e protein were applied to a Superdex 200 column (GE Healthcare) for purification to homogeneity. For the crystallization of Shb1e protein, crystals of Shb1e-containing compound **2** were grown by the vapor diffusion method with PEG 2000 monomethyl ether as a precipitant at 20 °C. An equal volume of well liquor containing PEG (14%), MES (pH 6.5, 100 mM), and ZnSO₄ (10 mM) was mixed with protein solution (5 mg mL⁻¹) containing compound **2** (3 mM).

Data collection and structure analysis of Shb1e protein: X-ray diffraction measurements were performed in BL26B2 at SPring-8 (RIKEN). Diffraction images of the dataset were indexed, integrated, and scaled by use of the HKL2000 program suite.^[41] Further processing was carried out by use of the CCP4 package.^[42] The data col-

lection and refinement statistics are summarized in Table S2. The crystal belongs to the space group $P2_12_12_1$, with unit cell dimensions of $a = 40.0 \text{ \AA}$, $b = 53.9 \text{ \AA}$, and $c = 125.5 \text{ \AA}$.

Multiwavelength anomalous dispersion data of Shble protein in complex with compound **2** were measured at the absorption edge of the Cu atom. The determination of the copper position and initial phasing were performed by use of the AUTOSHARP program.^[43] The initial phases were improved, and the models in the electron density map were built with the LAFIRE program.^[44] The protein/compound **2** model was then constructed manually with the aid of the XtalView program.^[45] Crystallographic refinement was performed by use of the crystallography and NMR system.^[46] The crystallographic coordinates of Shble protein in complex with compound **2** have been deposited at the Protein Data Bank (PDB ID: 2ZHP).

Compound characterization: The structure of each compound that was stored in a compound library was further confirmed by examination of spectra data. An LTQ Orbitrap mass spectrometer (Thermo Fisher Scientific, Waltham, MA) was used for ESI. IR spectra were recorded on an FT-2100 instrument (Horiba, Kyoto, Japan). UV spectra were recorded on a Hitachi U-2800 (Hitachi, Tokyo, Japan) instrument.

Bleomycin derivative 1: IR (KBr): $\tilde{\nu} = 3350, 2935, 1720, 1640, 1555, 1065 \text{ cm}^{-1}$; UV/Vis (1% 1 cm): $\lambda_{\text{max}} (\epsilon) = 599 (0.52), 332 \text{ sh} (14.8), 311 \text{ sh} (58.6), 293 (85.0), 245 \text{ sh} (109), 212 \text{ nm sh} (242 \text{ mol}^{-1} \text{ dm}^3 \text{ cm}^{-1})$; HRMS (ESI+): m/z : calcd for $\text{C}_{72}\text{H}_{116}\text{N}_{22}\text{O}_{21}\text{S}_2\text{Cu}$: 875.8706 $[M]^{2+}$; found: 875.8717.

Bleomycin derivative 4: IR (KBr): $\tilde{\nu} = 3390, 2935, 1720, 1645, 1560, 1065 \text{ cm}^{-1}$; UV/Vis (1% 1 cm): $\lambda_{\text{max}} (\epsilon) = 596 (0.60), 332 \text{ sh} (16.8), 311 \text{ sh} (65.2), 293 (94.0), 244 (121), 211 \text{ nm sh} (230 \text{ mol}^{-1} \text{ dm}^3 \text{ cm}^{-1})$; HRMS (ESI+): m/z : calcd for $\text{C}_{62}\text{H}_{98}\text{N}_{20}\text{O}_{22}\text{S}_2\text{Cu}$: 800.7945 $[M]^{2+}$; found: 800.7953.

Bleomycin derivative 6: IR (KBr): $\tilde{\nu} = 3380, 2935, 1715, 1650, 1535, 1065 \text{ cm}^{-1}$; UV/Vis (1% 1 cm): $\lambda_{\text{max}} (\epsilon) = 594 (0.64), 332 \text{ sh} (17.6), 312 \text{ sh} (77.2), 289 (132), 249 (134), 211 \text{ nm sh} (241 \text{ mol}^{-1} \text{ dm}^3 \text{ cm}^{-1})$; HRMS (ESI+): m/z : calcd for $\text{C}_{59}\text{H}_{84}\text{N}_{18}\text{O}_{21}\text{S}_2\text{Cu}$: 753.7374 $[M]^{2+}$; found: 753.7392.

Bleomycin derivative 12: IR (KBr): $\tilde{\nu} = 3335, 2940, 1720, 1671, 1637, 1525, 1050 \text{ cm}^{-1}$; UV/Vis (1% 1 cm): $\lambda_{\text{max}} (\epsilon) = 599 (0.92), 332 \text{ sh} (24.0), 313 \text{ sh} (60.2), 301 (66.2), 246 (118), 213 \text{ nm sh} (145 \text{ mol}^{-1} \text{ dm}^3 \text{ cm}^{-1})$; HRMS (ESI+): m/z : calcd for $\text{C}_{37}\text{H}_{56}\text{N}_{12}\text{O}_{19}\text{Cu}$: 1036.3153 $[M]^+$; found: 1036.3134.

Acknowledgements

We would like to thank I. Matsuo, A. Asami, N. Ikeda, Y. Kondoh, and Y. Ito for valuable suggestions. We also thank M. Yamamoto, RIKEN SPring-8 Center, and H. Miyatake, RIKEN, for data collection at SPring-8. The synchrotron radiation experiments were performed at the BL26B2 in SPring-8 with the Mail-in data collection system. This study was supported in part by Grants-in-Aid for Scientific Research on Priority Areas "Life surveyor" from the Ministry of Education, Culture, Sports, Science and Technology of Japan (Nos. 18038044 and 19021005 to S.S. and N.K.), the Chemical Biology Project (RIKEN), and the Special Postdoctoral Researchers Program (H.O.).

Keywords: arrays • bleomycins • photochemistry • Shble protein • structure–activity relationships

- [1] H. Umezawa, K. Maeda, T. Takeuchi, Y. Okami, *J. Antibiot.* **1966**, *19*, 200–209.
- [2] M. Ishizuka, H. Takayama, T. Takeuchi, H. Umezawa, *J. Antibiot.* **1967**, *20*, 15–24.
- [3] T. Takita, Y. Muraoka, T. Nakatani, A. Fujii, Y. Umezawa, H. Naganawa, *J. Antibiot.* **1978**, *31*, 801–804.
- [4] T. Takita, Y. Umezawa, S. Saito, H. Morishima, H. Umezawa, Y. Muraoka, M. Suzuki, M. Otsuka, S. Kobayashi, M. Ohno, *Tetrahedron Lett.* **1981**, *22*, 671–674.
- [5] T. Takita, Y. Umezawa, S. Saito, H. Morishima, H. Naganawa, H. Umezawa, T. Tsuchiya, T. Miyake, S. Kageyama, S. Umezawa, Y. Muraoka, M. Suzuki, M. Otsuka, M. Narita, S. Kobayashi, M. Ohno, *Tetrahedron Lett.* **1982**, *23*, 521–524.
- [6] Y. Aoyagi, K. Katano, H. Suguna, J. Primeau, L. H. Chang, S. M. Hecht, *J. Am. Chem. Soc.* **1982**, *104*, 5537–5538.
- [7] T. Yamamoto, *Br. J. Dermatol.* **2006**, *155*, 869–875.
- [8] H. Umezawa, *Fed. Proc.* **1974**, *33*, 2296–2302.
- [9] E. Sausville, J. Peisach, S. Horwitz, *Biochem. Biophys. Res. Commun.* **1976**, *73*, 814–822.
- [10] M. Sugiyama, T. Kumagai, H. Matsuo, M. Bhuiyan, K. Ueda, H. Mochizuki, N. Nakamura, J. Davies, *FEBS Lett.* **1995**, *362*, 80–84.
- [11] M. Sugiyama, C. J. Thompson, T. Kumagai, K. Suzuki, R. Deblaere, R. Vilarroel, J. Davies, *Gene* **1994**, *151*, 11–16.
- [12] A. Gattignol, H. Durand, G. Tiraby, *FEBS Lett.* **1988**, *230*, 171–175.
- [13] D. Drocourt, T. Calmels, J. Reynes, M. Baron, G. Tiraby, *Nucleic Acids Res.* **1990**, *18*, 4009.
- [14] M. Z. A. Bhuiyan, K. Ueda, Y. Inouye, M. Sugiyama, *Appl. Microbiol. Biotechnol.* **1995**, *43*, 65–69.
- [15] T. Kumagai, T. Nakano, M. Maruyama, H. Mochizuki, M. Sugiyama, *FEBS Lett.* **1999**, *442*, 34–38.
- [16] J. Weinbach, A. Camus, J. Barra, P. Dumont, M. Julian, S. Cros, C. Babinet, G. Tiraby, *Cancer Res.* **1996**, *56*, 5659–5665.
- [17] P. L. Tran, J. Weinbach, P. Opolon, G. L. -Cruz, J.-P. Reynes, A. Grégoire, E. Kremer, H. Durand, M. Perricaudet, *J. Clin. Invest.* **1997**, *99*, 608–617.
- [18] N. Kanoh, S. Kumashiro, S. Simizu, Y. Kondoh, S. Hatakeyama, H. Tashiro, H. Osada, *Angew. Chem.* **2003**, *115*, 5742–5745; *Angew. Chem. Int. Ed.* **2003**, *42*, 5584–5587.
- [19] N. Kanoh, A. Asami, M. Kawatani, K. Honda, S. Kumashiro, H. Takayama, S. Simizu, T. Amemiya, Y. Kondoh, S. Hatakeyama, K. Tsuganezawa, R. Ueda, A. Tanaka, S. Yokoyama, H. Tashiro, H. Osada, *Chem. Asian J.* **2006**, *1*, 789–797.
- [20] N. Kanoh, T. Nakamura, K. Honda, H. Yamakoshi, Y. Iwabuchi, H. Osada, *Tetrahedron* **2008**, *64*, 5692–5698.
- [21] J. Bradner, O. McPherson, R. Mazitschek, D. Barnes-Seeman, J. Shen, J. Dhaliwal, K. Stevenson, J. Duffner, S. Park, D. Neuberger, P. Nghiem, S. Schreiber, A. Koehler, *Chem. Biol.* **2006**, *13*, 493–504.
- [22] I. Miyazaki, S. Simizu, H. Ichimiya, M. Kawatani, H. Osada, *Biosci. Biotechnol. Biochem.* **2008**, *72*, 2739–2749.
- [23] M. Platz, A. S. Admasu, S. Kwiatkowski, P. J. Crocker, N. Imai, D. S. Watt, *Bioconjugate Chem.* **1991**, *2*, 337–341.
- [24] M. Maruyama, T. Kumagai, Y. Matoba, M. Hayashida, T. Fujii, Y. Hata, M. Sugiyama, *J. Biol. Chem.* **2001**, *276*, 9992–9999.
- [25] T. Takita, Y. Muraoka, T. Nakatani, A. Fujii, Y. Itaka, H. Umezawa, *J. Antibiot.* **1978**, *10*, 1073–1077.
- [26] P. Dumas, M. Bergdoll, C. Cagnon, J. Masson, *EMBO J.* **1994**, *13*, 2483–2492.
- [27] S. Brouns, H. Wu, J. Akerboom, A. Turnbull, W. de Vos, J. van der Oost, *J. Biol. Chem.* **2005**, *280*, 11422–11431.
- [28] A and B indicate each subunit of the Shble dimer complex. For example, Phe33B means the Phe33 residue of subunit B of the Shble protein.
- [29] M. Sugiyama, T. Kumagai, M. Hayashida, M. Maruyama, Y. Matoba, *J. Biol. Chem.* **2002**, *277*, 2311–2320.
- [30] Y. Kawano, T. Kumagai, K. Muta, Y. Matoba, J. Davies, M. Sugiyama, *J. Mol. Biol.* **2000**, *295*, 915–925.
- [31] C. Vanbelle, B. Brutscher, M. Blackledge, C. Muhle-Goll, M. Rémy, J. Masson, D. Marion, *Biochemistry* **2003**, *42*, 651–663.

- [32] U. Galm, M. Hager, S. Van Lanen, J. Ju, J. Thorson, B. Shen, *Chem. Rev.* **2005**, *105*, 739–758.
- [33] Q. Ma, Z. Xu, B. R. Schroeder, W. Sun, F. Wei, S. Hashimoto, K. Konishi, C. T. Leitheiser, S. M. Hecht, *J. Am. Chem. Soc.* **2007**, *129*, 12439–12452.
- [34] Y. Muraoka, M. Suzuki, A. Fujii, Y. Umezawa, H. Naganawa, T. Takita, H. Umezawa, *J. Antibiot.* **1981**, *34*, 353–357.
- [35] H. Umezawa, Y. Takahashi, A. Fujii, T. Saino, T. Shirai, *J. Antibiot.* **1973**, *26*, 117–119.
- [36] A. Fujii, T. Takita, K. Maeda, H. Umezawa, *J. Antibiot.* **1973**, *26*, 398–399.
- [37] H. Umezawa, *Pure Appl. Chem.* **1971**, *28*, 665–680.
- [38] T. Takita, Y. Muraoka, T. Yoshioka, A. Fujii, K. Maeda, *J. Antibiot.* **1972**, *25*, 755–757.
- [39] K. Kasai, H. Naganawa, T. Takita, H. Umezawa, *J. Antibiot.* **1978**, *31*, 1316–1320.
- [40] H. Umezawa, Y. Takahashi, A. Fujii, T. Saino, T. Shirai, *J. Antibiot.* **1973**, *26*, 117–119.
- [41] Z. Otwinowski, W. Minor, *Methods Enzymol.* **1997**, *276*, 307–326.
- [42] Collaborative Computational Project, Number 4, *Acta Crystallogr. Sect. D Biol. Crystallogr.* **1994**, *50*, 760–763.
- [43] E. de La Fortelle, G. Bricogne, *Methods Enzymol.* **1997**, *276*, 472–494.
- [44] M. Yao, Y. Zhou, I. Tanaka, *Acta Crystallogr. Sect. D Biol. Crystallogr.* **2006**, *62*, 189–196.
- [45] D. E. McRee, *J. Struct. Biol.* **1999**, *125*, 156–165.
- [46] A. T. Brünger, P. D. Adams, G. M. Clore, W. L. DeLano, P. Gros, R. W. Grosse-Kunstleve, J. S. Jiang, J. Kuszewski, M. Nilges, N. S. Pannu, R. J. Read, L. M. Rice, T. Simonson, G. L. Warren, *Acta Crystallogr. Sect. D Biol. Crystallogr.* **1998**, *54*, 905–921.

Received: November 6, 2008

Published online on February 16, 2009